INTERACTION OF 42-MeV ALPHA PARTICLES WITH HELIUM-3

by John S. Vincent and Edmund T. Boschitz

Lewis Research Center
Cleveland, Ohio

0132012

1. Report No. NASA TN D-5530	2. Government Accession No.	3. Recipient's Catalog No.
4. Title and Subtitle INTERACTION OF 42-MeV ALPHA PARTICLES WITH HELIUM-3		5. Report Date November 1969
		6. Performing Organization Code
7. Author(s) John S. Vincent and Edmund T. Boschitz		8. Performing Organization Report No. E-5234
9. Performing Organization Name and Address Lewis Research Center National Aeronautics and Space Administration Cleveland, Ohio 44135		10. Work Unit No. 129-02
		11. Contract or Grant No.
		13. Type of Report and Period Covered
12. Sponsoring Agency Name and Address National Aeronautics and Space Administration Washington, D.C. 20546		Technical Note
		14. Sponsoring Agency Code

15. Supplementary Notes

16. Abstract

The center-of-mass differential cross section for the elastic scattering of 42-MeV alpha particles from ^{3}He was measured between 20° and 160°. Nonelastic events were integrated to estimate the total reaction cross section. Differential cross sections for ^{3}He$(\alpha, p)^6$Li to the ground and first excited states were measured between 20° and 160°. An optical model description of the elastic data gives a satisfactory description if the absorptive potential is radially extended beyond the real potential. The reaction cross sections are qualitatively described by the distorted-wave Born approximation theory.

17. Key Words (Suggested by Author(s)) Differential cross sections ^{3}He$(\alpha, \alpha)^3$He, ^{3}He$(\alpha, p)^6$Li for E_α = 42 MeV	18. Distribution Statement Unclassified - unlimited		
19. Security Classif. (of this report) Unclassified	20. Security Classif. (of this page) Unclassified	21. No. of Pages 20	22. Price* $3.00

*For sale by the Clearinghouse for Federal Scientific and Technical Information
Springfield, Virginia 22151

INTERACTION OF 42-MeV ALPHA PARTICLES WITH HELIUM-3

by John S. Vincent and Edmund T. Boschitz

Lewis Research Center

SUMMARY

The center-of-mass differential cross section for elastic and nonelastic scattering of 42-MeV alpha particles from ^{3}He was measured between 20° and 160°. A phenomenological description of the elastic data is given by an optical model calculation. It was found that to reproduce the shape of the data the absorptive potential must extend radially beyond the real potential. Including a small spin-orbit potential in the calculation improves the comparison with the experiment and predicts a polarization which is consistent with one measurement at a nearby energy. The reaction cross section given by the optical model calculation is close to a minimum value estimated from integration of observed inelastic events.

The two-body reactions ^{3}He$(\alpha, p)^6$Li, ground and first excited states, were measured between 20° and 160° (center of mass). Optical potentials determined from elastic scattering data were used in a distorted-wave Born approximation prediction for these cross sections. Qualitative agreement was obtained assuming only the ^{3}He stripping mode.

INTRODUCTION

The interaction of ^{3}He with ^{4}He presents an interesting problem in the study of few-nucleon systems. The elastic scattering has been studied for energies to 23.6 MeV (refs. 1 to 8) in the center-of-mass system. At low energies, phase-shift analysis (ref. 8) can yield excellent descriptions of the cross sections while giving much information concerning states of the compound system. This technique has been exploited to center-of-mass energies of 10.3 MeV, assuming that only two-body reactions leading to p + ^{6}Li contribute to the imaginary phase shifts. At higher energies this would probably be a poor assumption because of the onset of multibody reactions. A second approach has been the synthesis of an effective interaction from two-body potentials

through use of the method of resonating groups (refs. 9 and 10). This method has been used for center-of-mass energies to 18 MeV. The shape of the elastic differential cross section is quite well predicted, but the calculation at 18 MeV greatly overestimates the magnitude, probably because of the neglect of inelastic channels. A third theoretical technique is the application of the conventional optical model to the 18-MeV center-of-mass data (ref. 11) of Birmingham. The unsuccessful attempts to fit this data by Hodgson (ref. 12) led to consideration of spectator exchange terms in the amplitude. The result of these calculations, however, was only qualitative agreement with experiment. In all these studies the spin-orbit part of the scattering potential was neglected. Although there are indications (refs. 13 to 15) that this potential is small, the extent to which effects on the cross section are manifested is not known.

The purpose of the work reported herein is to provide a more complete experimental picture of the interaction of ^{3}He with ^{4}He at 18 MeV. This included a more precise elastic differential cross section, an estimate of the lower limit of total reaction cross section, and measurement of the prominent two-body reactions. These data were analyzed using the optical model and the distorted-wave Born approximation. In the analysis of elastic scattering, the effects of adding a spin-orbit potential were investigated and the results are compared with our earlier polarization measurement (ref. 15).

EXPERIMENTAL PROCEDURE

The 42-MeV alpha-particle beam of the Lewis Research Center cyclotron was focused onto a ^{3}He gaseous target located at the center of a 1.5-meter scattering chamber. The target container was a 10-centimeter-diameter cylinder having windows of 2.5-μm Havar. The pressure was about 1/4 atmosphere, and it was continuously monitored by an electrical transducer which was accurate to ±1 torr. The temperature was constant during the experiment to within 1^O C. Mass analysis of the contents of the target before and after the experiment indicated less than 5 parts per thousand contaminant, mostly ^{4}He. The beam spot at the target was 3 millimeters in diameter with a divergence of about 9 milliradians. Integration of the incident beam current was judged to be accurate to about 1 percent. The direction of the beam was determined to within 0.1^O by measurement of the scattering yield at several small angles both to the right and left. The particle detection system consisted of an E-ΔE silicon counter telescope and an electronic device of the type designed by Goulding (ref. 16), which separates reaction products by mass. The angular resolution of the telescope was 0.73^O half width. The data were corrected for lost counts caused by electronic dead time.

The raw scattering data were analyzed by least-square fitting of the spectra. A typical spectrum for the reaction ^{3}He(α, p)^{6}Li is shown in figure 1. The two data peaks

correspond to protons which leave ^{6}Li in the ground and first excited states. Since the excited state near channel 25 is above the threshold for ^{6}Li breakup into ^{4}He + D, there is a continuum of protons below the data. The extraction of the integrated number of counts in this peak was accomplished by the following procedure. First, the ground-state peak (near channel 45) was fitted by a skewed Gaussian function in which the skewness and width were allowed to vary. Once the shape of this typical peak had been determined, this shape was reintroduced as a fixed parameter for fitting of the excited state. This procedure eliminates, to a large extent, the distortion of this peak caused by the underlying proton continuum, the gross subtraction of which is approximated by an arbitrary logarithmic function (dashed line in fig. 1). The results of this procedure are indicated by the solid curve in figure 1, which is thought to be accurate to better than 10 percent. Data extracted are used to compute the center-of-mass differential cross sections given in tables I and II.

ANALYSIS OF ELASTIC SCATTERING

Certainly one of the simplest, but perhaps not the most lucid, description of ^{3}He-^{4}He scattering at these energies is provided by the optical model. The number of parameters necessary to describe the data is quite few compared to a phase-shift analysis, and the reaction cross section is easily introduced through use of the absorptive potential. The latter device is probably a better approximation to reality at 18 MeV than the neglect of reaction channels, as in the resonating group approach (ref. 10). This is true because the energy is much higher than required for the disintegration of ^{3}He into p + d(Q = 5.4 MeV) and p + p + n(Q = 7.7 MeV). For these reasons, the usual optical model was employed. A modified version of the computer program (ref. 17) SCAT 4 was used. The potentials were local, with the real part having the conventional Woods-Saxon form factor. Various different shapes were employed for the absorptive potential, and the spin-orbit term was of the Thomas type. All parameters of the potentials could be varied automatically by a search routine (ref. 18) so as to obtain the best fit to the experimental data.

The result of the first optical model search is shown, together with the experimental data, in figure 2. The initial parameters were those of Tang, Schmid, and Wildermuth (ref. 9); the real and absorptive form factors were the same and of the Woods-Saxon type. The resulting curve (similar to theirs) does not give a good description of the data, especially at scattering angles greater than 100°. The reaction cross section predicted was 100 millibarns. This value was judged to be more than an order of magnitude too low by using the following arguments. All reactions except those leading to p + ^{6}Li have a scattered alpha particle as one of the products. Therefore, integration of the

complete inelastic alpha-particle spectrum over all energies and angles and addition of the p + ^{6}Li reaction cross sections should yield the total reaction cross section. As an approximation, certainly giving a lower limit to this cross section, the inelastic portion of the experimental alpha spectrum was integrated for $E_\alpha \geq 17$ MeV and the cross section computed for a series of angles. The result is shown in figure 3, together with a reasonable extrapolation to zero scattering angle. This curve was integrated, yielding a value of 1260 millibarns. The p + ^{6}Li reaction cross sections of 100 millibarns are small by comparison, but the minimum value of the total reaction cross section must be greater than 1300 millibarns.

To try to resolve the discrepancy between the first optical model prediction of 100 millibarns and our estimate, another approach was attempted. The real and imaginary potential form factors in the optical model were allowed to vary independently. A considerable improvement was achieved. Figure 4 shows the results of several computer searches, each starting with a different absorptive form factor. Figure 5 shows a calculation similar to those in figure 4 but having a real potential which is about a factor of 2 deeper. All these computations predict a total reaction cross section between 1100 and 1200 millibarns, which is close to our estimate of a lower limit. An interesting point is that although the three absorptive form factors differ greatly, they have in common a large radial extension beyond the real potential. In fact, if an attempt is made to force the absorptive radius to smaller values, the search program increases the depth and diffuseness to produce roughly the same amount of absorption at a large radius. The relation between these variables for a constant standard deviation is shown in figure 6.

Finally, the effect of adding a small spin-orbit potential was investigated. The principal result was to decrease the depth of the second minimum in the elastic cross section so as to bring the calculations closer to the data, as shown by the solid curve in figure 7 for potential set I (table III). Figure 7 also shows a calculation using potential set II (table III); both the shallow and deep real potential solutions are given, as there is some question as to which is more desirable for reaction theory calculations. The description of the data is quite good in both cases.

Further investigation revealed that use of a spin-orbit potential larger than about 1 MeV impaired both fits to the cross section. Also, it should be noted that the spin-orbit potential was taken to be attractive, as in proton scattering. However, the sign of the spin orbit potential is not known for the ^{3}He-^{4}He interaction, as the earlier experiment (ref. 15) measured only the magnitude of polarization. But the small values of the spin-orbit potential are in general agreement with other work (refs. 13 and 14) on the elastic scattering of polarized ^{3}He.

^{3}He$(\alpha, p)^6$Li REACTIONS

The prominent two-body reactions going to $p + {}^6$Li in the ground state (Q = -4.02 MeV) and first excited state (Q = -6.20 MeV) were observed. The first of these transitions has been studied by using 17-MeV protons (ref. 19) for the time-reversed reaction. An important fact for the ^{3}He(α, p) reaction is that at 18 MeV (center of mass) the energy is about 1 MeV below that necessary to extract a proton from the incident alpha particle. Therefore, it would be expected that target (^{3}He) stripping and proton knockout from ^{3}He would be favored. The experimental data shown in figures 8 and 9 indicate an enhancement of large-angle scattering which is indicative of target stripping.

There are several difficulties which are encountered in making a theoretical calculation for these reactions; some can be classified as computational complexities and others are more intrinsic in nature. In the first place, most Born approximation calculations assume one reaction mechanism to the exclusion of others. This probably is not realistic for ^{3}He$(\alpha, p)^6$Li reactions. In the case of target stripping the interaction is caused by the d-p potential, whereas for knockout the α-p potential is used. Certainly, neither of these processes can be excluded. Hird (ref. 20) has studied the ^{12}C$(\alpha, p)^{15}$N reaction including both stripping and knockout in the plane-wave approximation. The comparison with data gave only qualitative agreement. In the distorted-wave formalism, Hird (ref. 20) and Edwards (ref. 21) point out that knockout or stripping is excluded depending on the definition of the distorted waves, but they suggest that this is primarily a computational difficulty. In this work, the distorted-wave theory (ref. 22) is used, assuming only the stripping mechanism.

Another problem encountered with the distorted-wave formalism is connected with the use of optical potentials. Both knockout and stripping matrix elements have terms which are neglected by assuming a heavy core nucleus. In essence, the theory (ref. 23) approximates the exit particle-core interaction by the exit-channel optical potential. This is a poor approximation for light targets, and the correct calculation involves quite some mathematical difficulty (ref. 23). In the case of ^{3}He(α, p)Li^6 this corresponds to neglecting the term containing $V_{\alpha-p} - \overline{V}_{Li-p}$; this approximation was made herein. For the entrance channel the optical potential used was the second set from table III, and for the p - ^{6}Li channel a separate calculation was made on the 19-MeV proton scattering from ^{6}Li of Vanetsian et al. (ref. 24). The results are shown in figure 10.

Finally, direct reaction amplitudes contain the bound-state wave-functions. For a light nucleus, such as ^{6}Li, some crude approximations are usually made; for instance, an alpha-particle core with individual nucleons or a cluster moving in orbit about it. If the reaction occurs primarily at the nuclear surface, this kind of approximation might be valid because the asymtotic form of the wave function at large radii is not sensitive

to the internal structure. (Of course, the absolute magnitude of the computed cross section will be sensitive to different wave functions used even though the shape is not.)

For the ground-state transition, a deuteron from ^{3}He was assumed to be captured into an s-state orbit about an alpha-particle core. The eigenenergy of the bound state was -1.50 MeV, the deuteron separation energy. These calculations are shown in figure 8. The dashed curve considers reactions which occur throughout the target volume, whereas the solid curve is for reactions which take place in the nuclear surface, at radii greater than 4 fermi. This radius was chosen empirically, for the best match at large angles. The deep minima in all the calculations are not in agreement with the data; however, the cutoff calculation, indicating surface reaction, seems to be in better agreement than the noncutoff curve, especially in the stripping peak. The situation is somewhat improved if some capture into a d-state orbit is included. This is allowed from spin and parity considerations. The dot-dashed curve in figure 8 shows the results of equal amounts of d- and s-state capture. The amplitudes were added coherently and the squares summed over magnetic quantum numbers.

The cross section for transition to the first excited state in ^{6}Li is interesting because this level is unstable for decay into ^{4}He + D by about 1 MeV. The level width (ref. 25) determined from inelastic proton and deuteron scattering is 25 keV, corresponding to a lifetime of 2.6×10^{-20} second, which is long compared to incident particle transit time across the nucleus. Although our direct reaction code does not consider transitions to unbound states, it seems reasonable that a weakly bound particle wave function might be a good approximation, if the level width is narrow enough. A series of stripping calculations was made, therefore, using as a model a weakly bound final state having the deuteron in a d-orbit. Figure 9 shows three theoretical curves. The dashed curve is for reactions throughout the nuclear volume. This shape does not differ for "pseudo" binding energies of 0.8, 0.5, or 0.09 MeV. The solid and dot-dashed curves are radial cutoff calculations for the same surface region as used for the ground-state calculations. The binding energies were 0.5 and 0.09 MeV, respectively. Although the models used are extremely crude, the description of the data in the stripping peak is quite good, and this may indicate some measure of validity for the assumptions.

CONCLUSIONS

An optical model description for the elastic scattering of ^{4}He from ^{3}He gives a good description of the data at 18 MeV (center of mass), provided a rather large radial extention of the absorptive potential is assumed. Within the framework of the optical model, this assumption is necessary to provide a large reaction cross section in agreement with the experimental estimate of its lower limit. Addition of a small spin-orbit

potential improves the calculated differential cross section and predicts a polarization which is consistent with a previous measurement. The two-body reactions leading to p + ^{6}Li can be qualitatively described by a direct reaction calculation assuming stripping of a deuteron from ^{3}He into s- and d-state orbitals about the incident alpha particle.

Lewis Research Center,
    National Aeronautics and Space Administration,
        Cleveland, Ohio, September 4, 1969,
            129-02.

REFERENCES

1. Barnard, A. C. L.; Jones, C. M.; and Phillips, G. C.: The Scattering of He^3 by He^4. Nucl. Phys., vol. 50, 1964, pp. 629-640.

2. Miller, Philip D.; and Phillips, G. C.: Scattering of He^3 from He^4 and States in Be^7. Phys. Rev., vol. 112, no. 6, Dec. 15, 1958, pp. 2048-2052.

3. Phillips, G. C.; and Miller, P. D.: Measurement of Spin Polarization by Nuclear Scattering. Phys. Rev., vol. 115, no. 5, Sept. 1, 1959, pp. 1268-1270.

4. Tombrello, T. A.; and Parker, P. D.: Scattering of He^3 from He^4. Phys. Rev., vol. 130, no. 3, May 1, 1963, pp. 1112-1119.

5. Chiba, R.; et al: He^3-Alpha Scattering. J. Phys. Soc. Japan, vol. 16, no. 6, June 1961, pp. 1077-1085.

6. Jacobs, Clarence G.; and Brown, Ronald E.: Elastic Scattering of He^3 by He^4 from 17.8 to 30.0 MeV. Bull. Am. Phys. Soc., Ser. II, vol. 12, no. 8, Dec. 1967, p. 1175.

7. Cahill, Thomas A.; and Martens, P. C.: Differential Cross Section of ^{3}He(α, α)^{3}He between 43.4 and 58.2 MeV. Bull. Am. Phys. Soc., Ser. II, vol. 14, no. 4, Apr. 1969, p. 553.

8. Spiger, R. J.; and Tombrello, T. A.: Scattering of He^3 by He^4 and of He^4 by Tritium. Phys. Rev., vol. 163, no. 4, Nov. 20, 1967, pp. 964-984.

9. Tang, Y. C.; Schmid, E.; and Wildermuth, K.: Scattering of He^3 by Alpha Particles. Phys. Rev., vol. 131, no. 6, Sept. 15, 1963, pp. 2631-2641.

10. Brown, Ronald E.; and Tang, Y. C.: Study of $He^3 + He^4$ and $H^3 + He^4$ Systems with the Resonating-Group Method. Phys. Rev., vol. 176, no. 4, Dec. 20, 1968, pp. 1235-1245.

11. Bredin, D. J.; et al: The Scattering of 29 MeV ^{3}He-particles by ^{1}H, ^{2}H, ^{3}He and ^{4}He Nuclei. Proc. Roy. Soc. (London), Ser. A, vol. 258, no. 1293, Oct. 18, 1960, pp. 202-214.

12. Squires, E. J.; Forest, A. E.; and Hodgson, P. E.: The Effect of Spectator Exchange Terms in He^4-He^3 Scattering. Nucl. Phys., vol. 42, 1963, pp. 490-497.

13. Hutson, R. L.; et al: Polarization of ^{3}He Elastically Scattered by ^{12}C and the ^{3}He Spin-Orbit Optical Potential. Phys. Letters, vol. 27B, no. 3, June 24, 1968, pp. 153-155.

14. Patterson, D. M.; and Cramer, J. G.: An Estimate of the ^{3}He Spin-Orbit Potential from Spin-Flip Measurements. Phys. Letters, vol. 27B, no. 6, Aug. 19, 1968, pp. 373-375.

15. Boschitz, E. T.; and Vincent, J. S.: Polarization in ^{3}He-^{4}He Scattering Near 26 MeV. International Nuclear Physics Conference. Richard L. Becker, ed., Academic Press, 1967, pp. 1023-1024.

16. Goulding, Fred S.; Landis, Donald A.; Cerny, Joseph, III; and Pehl, Richard H.: A New Particle Identifier Technique for Z=1 and Z=2 Particles in the Energy Range > 10 MeV. IEEE Trans. Nucl. Sci., vol. NS-11, no. 3, June 1964, pp. 388-398.

17. Melkanoff, Michel A.; Saxon, David S.; Cantor, David G.; and Nodvik, John S.: A Fortran Program for Elastic Scattering Analyses with the Nuclear Optical Model. Publ. in Automatic Computation No. 1, Univ. California Los Angeles, 1961.

18. Davidon, William C.: Variable Metric Method for Minimization. Rep. ANL-5990 (Rev.), Argonne National Lab., Nov. 1959.

19. Likely, J. G.; and Brady, F. P.: Pickup Behavior in $Li^6(p, He^3)He^4$ and $F^{19}(p, \alpha)O^{16}$ at 18 MeV. Phys. Rev., vol. 104, no. 1, Oct. 1, 1956, pp. 118-123.

20. Hird, B.: The Direct Exchange Contributions to the Reaction $^{12}C(\alpha, p)^{15}N$ Between 20 MeV and 40 MeV. Nucl. Phys., vol. 86, 1966, pp. 268-278.

21. Edwards, Steve: Exchange Terms in Direct Nuclear Reaction Theories. Nucl. Phys,, vol. 47, 1963, pp. 652-670.

22. Gibbs, W. R.; et al: Direct Reaction Calculation. NASA TN D-2170, 1964.

23. Tobocman, W.: Theory of Direct Nuclear Reactions. Oxford Univ. Press, 1961, pp. 30-36.

24. Vanetsian, R. A.; Klyucharev, A. P.; and Fedchenko, E. D.: Investigation of the Differential Cross Section for Elastic Scattering of 19.6 MeV Protons on Separated Isotopes. Soviet J. At. Energy, vol. 6, no. 6, Dec. 1960, pp. 490-495.

25. Browne, C. P.; and Bockelman, C. K.: Comparison of Energy Levels of Li^6 from Various Reactions. Phys. Rev., vol. 105, no. 4, Feb. 15, 1957, pp. 1301-1306.

TABLE I. - EXPERIMENTAL DATA FOR ^{3}He(α,α)^{3}He

[$\dot{E}_{\alpha,\,lab}$, 42 MeV.]

Center-of-mass reaction angle, θ_{cm}, deg	Differential cross section, $d\sigma/d\Omega$, mb/sr	Statistical error, mb/sr	Center-of-mass reaction angle, θ_{cm}, deg	Differential cross section, $d\sigma/d\Omega$ mb/sr	Statistical error, mb/sr
25.·2	112.00	2.30	100.5	1.77	0.07
27.5	75.60	1.60	102.5	2.78	.10
29.9	47.30	1.00	104.5	4.16	.15
32.2	26.65	.60	106.5	6.66	.21
34.6	13.73	.30	108.5	8.75	.28
37.0	7.10	.17	110.5	11.20	.34
39.3	4.08	.10	112.5	13.15	.25
41.7	3.45	.09	114.5	14.49	.42
44.1	3.92	.10	116.5	15.20	.40
46.5	4.85	.13	118.5	14.85	.40
48.9	6.35	.15	120.5	14.80	.40
51.3	8.10	.19	122.5	13.50	.38
53.7	10.80	.24	124.5	11.80	.34
56.2	14.20	.30	126.5	10.10	.28
58.6	18.80	.41	128.5	8.33	.23
61.1	23.20	.30	130.5	6.78	.21
63.6	26.80	.53	132.5	4.85	.13
66.0	34.20	.75	134.5	3.54	.12
68.6	38.40	.81	136.5	2.42	.08
71.1	41.40	.86	138.5	2.01	.07
73.6	42.30	.90	140.5	1.18	.05
76.2	40.30	.90	142.5	1.24	.05
78.8	37.00	.85	144.5	1.54	.06
81.4	31.00	.50	146.5	1.99	.06
84.1	25.80	.51	148.5	2.73	.10
86.8	17.40	.43	150.5	3.86	.12
89.5	11.20	.26	152.5	5.55	.18
92.3	5.67	.16	154.5	8.25	.25
95.1	2.52	.09	156.5	11.70	.42
98.1	1.33	.05	158.5	15.50	.50

TABLE II. - EXPERIMENTAL DATA FOR ^{3}He(^{4}He, p)^{6}Li

$[E_{\alpha, \text{lab}}, \ 42 \text{ MeV.}]$

(a) Reaction Q-value, -4.02 MeV

(b) Reaction Q-value, -6.20 MeV

Center-of-mass reaction angle, θ_{cm}, deg	Differential cross section, $d\sigma/d\Omega$, mb/sr	Statistical error, mb/sr	Center-of-mass reaction angle, θ_{cm}, deg	Differential cross section, $d\sigma/d\Omega$, mb/sr	Statistical error, mb/sr
19.1	2.78	0.21	19.8	6.02	0.40
24.5	2.12	.10	25.2	5.29	.13
30.5	1.57	.07	31.5	4.71	.26
36.6	1.50	.07	43.9	3.92	.46
42.6	1.47	.08	50.0	4.06	.15
48.5	1.93	.10	56.0	3.60	.23
54.3	2.19	.11	62.0	3.26	.25
60.1	2.48	.13	67.9	3.04	.19
65.8	2.70	.18	73.6	3.20	.18
71.4	2.55	.09	76.5	3.62	.31
74.2	2.72	.15	82.1	3.67	.23
79.7	2.73	.20	87.6	3.69	.39
84.9	2.19	.16	98.1	4.26	.16
95.3	1.77	.10	103.2	4.36	.17
100.2	1.87	.11	108.3	4.56	.24
105.0	1.83	.11	115.0	4.92	.42
109.6	1.63	.14	127.6	6.09	.42
114.0	2.07	.15	136.7	8.02	.30
124.3	1.84	.13	144.7	11.2	.49
133.6	1.94	.14	151.6	14.9	1.01
141.7	1.85	.16	154.7	15.5	1.02
152.3	2.05	.19	157.6	17.6	.54
155.4	2.88	.22	163.0	19.4	1.10
161.2	4.20	.25	167.9	22.3	1.10
166.6	6.22	.27	172.4	23.8	2.10
171.5	7.32	.25			

TABLE III. - ^{3}He$(\alpha, \alpha)^3$He OPTICAL POTENTIALS

Potential set	Real potential, V, MeV	Radius of real potential, R_o, F	Diffuseness of real potential, A_o, F	Absorptive potential, W, MeV	Radius of absorptive potential, R_I, F	Diffuseness of absorptive potential, A_I, F	Spin-orbit potential, V_{so}, MeV	Radius of spin orbit potential, R_{so}, F	Diffuseness of spin orbit potential, A_{so}, F
I	65.7	2.22	0.27	0.75	5.5	1.68	0.50	2.22	0.27
II	173.0	2.28	.145	1.12	5.3	1.05	1.00	2.28	145
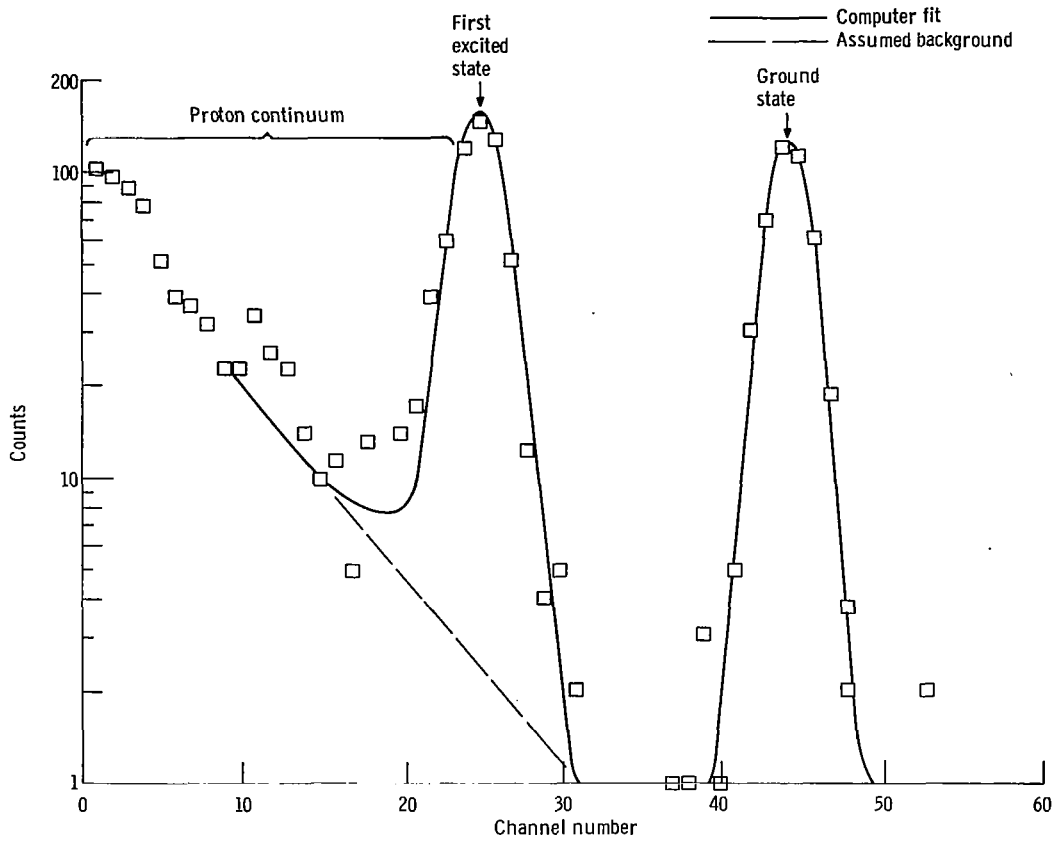
Figure 1. – Typical spectrum for ^{3}He$(\alpha, p)^6$Li. Laboratory scattering angle, $40°$.
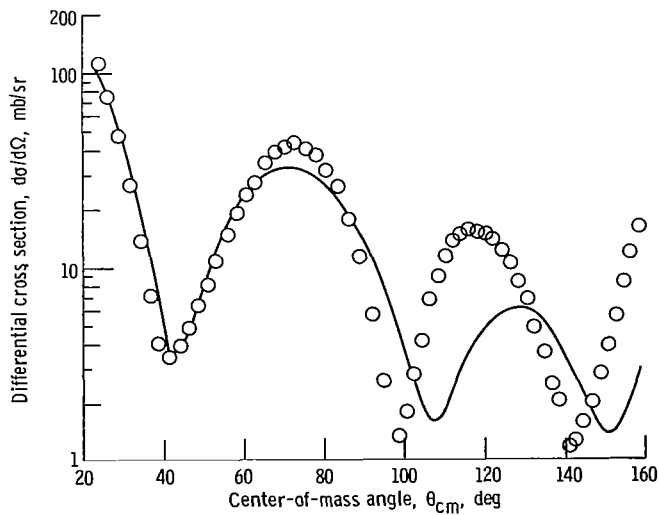
Figure 2. – Elastic scattering of 42-MeV alpha particles from helium-3.
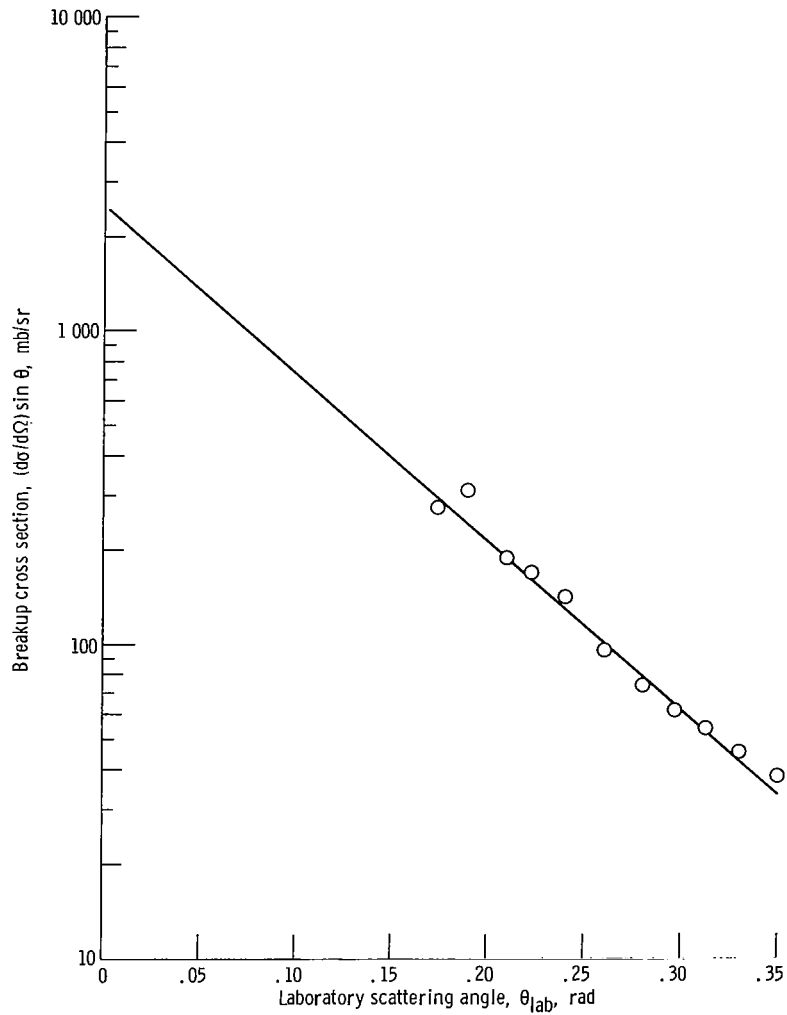
Figure 3. – Helium-3 breakup cross section having recoil alpha particles greater than 17 MeV; incident alpha energy, 42 MeV. $\frac{d\sigma}{d\Omega} \sin\theta = 2500\ e^{-12.5\ \theta}$; $\sigma_T = 2\pi \int_0^\theta \frac{d\sigma}{d\Omega} \sin\theta\ d\theta = 1260$ mb.
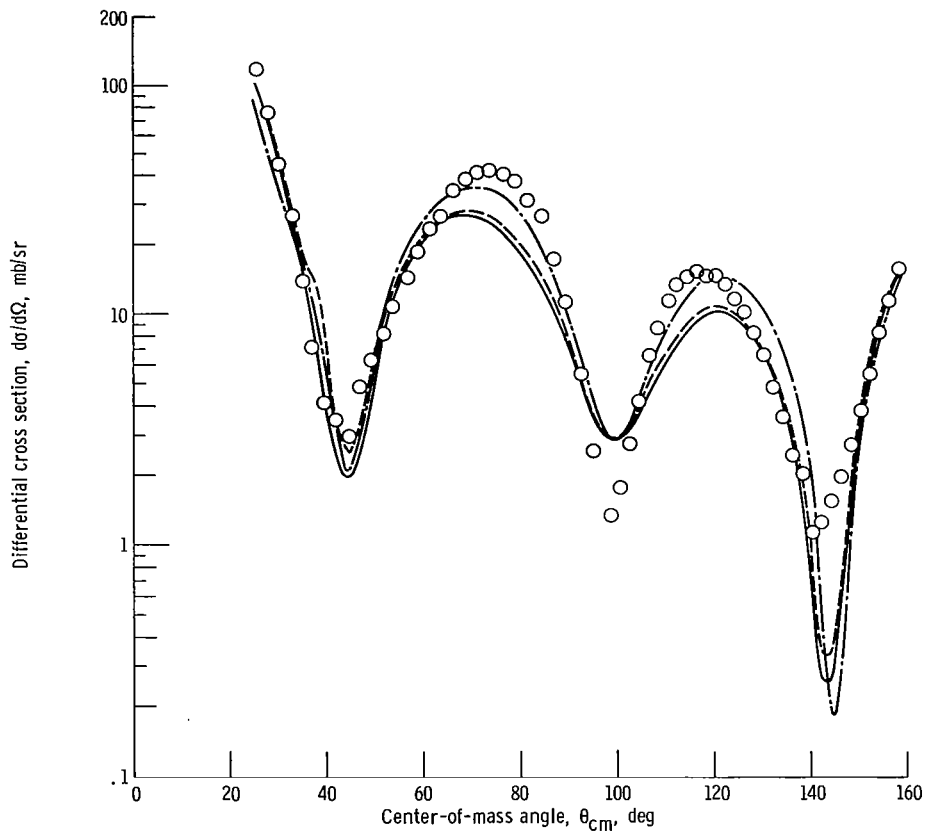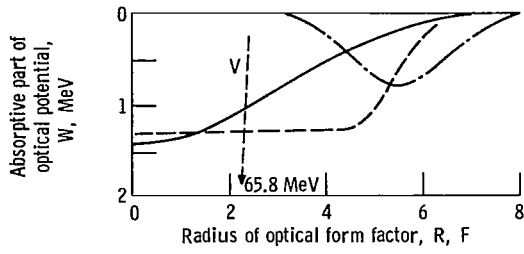
Figure 4. - Calculation of optical model having radially extended absorptive potentials. Real part of optical potential, 65.8 MeV; radius of optical form factor, 2.2 fermi; diffuseness, 0.27 fermi.

15
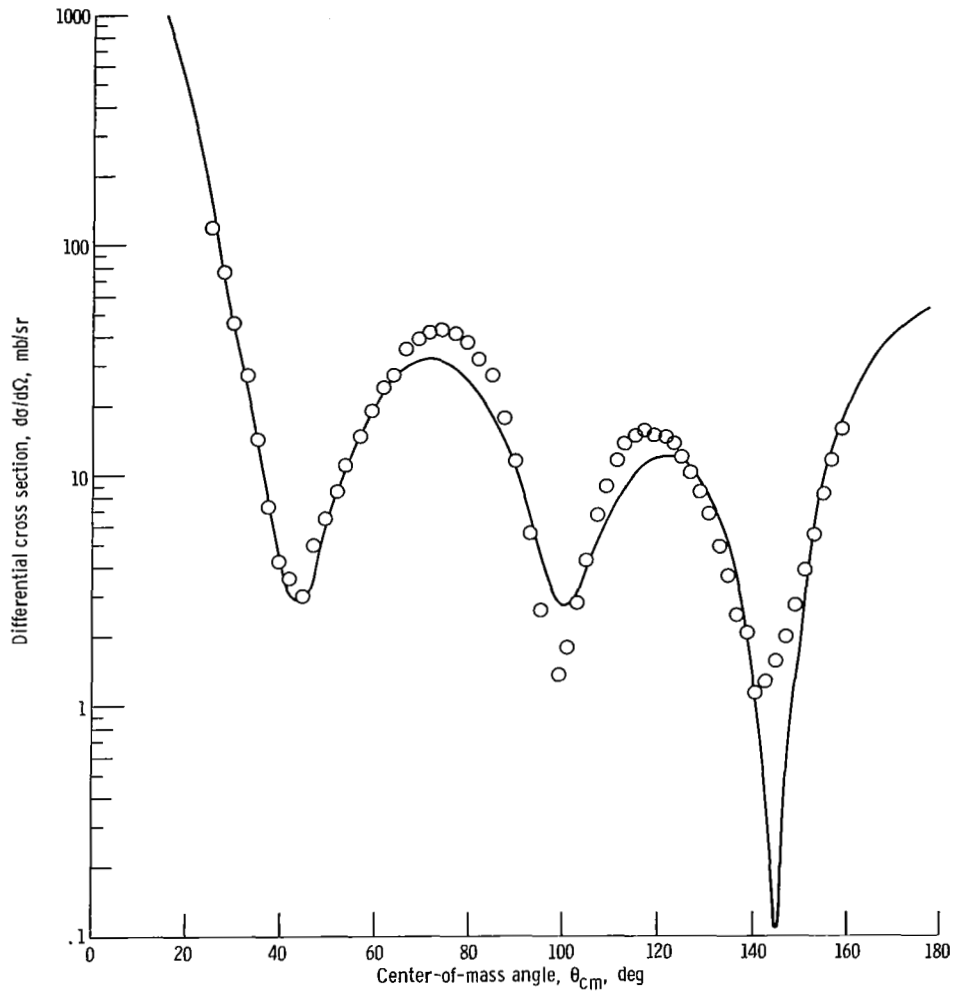
Figure 5. – Calculation of optical model having deep-well real potential and radially extended absorptive potential, using set II of table III.
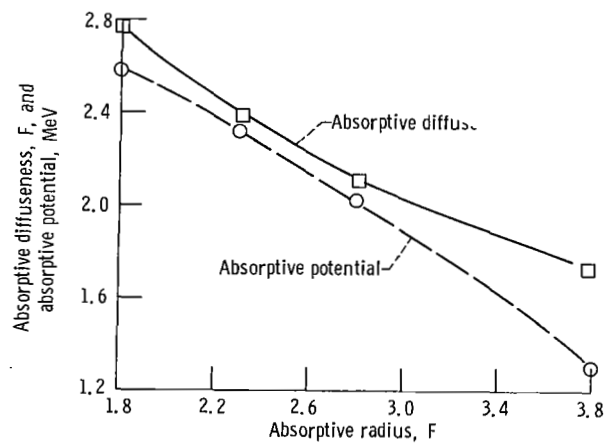
Figure 6. – Variation of absorptive well depth and diffuse-ness with radius for constant standard deviation from data (χ^2 = 800 for 60 points).

16
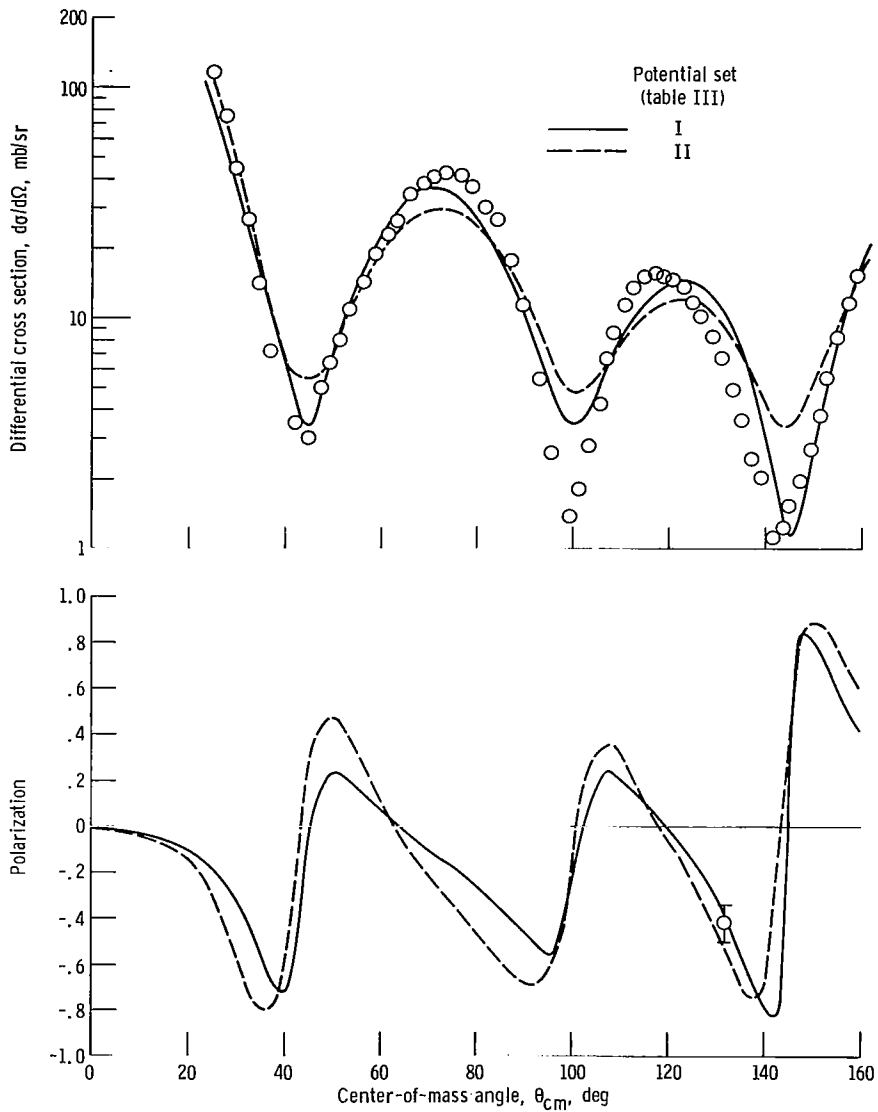
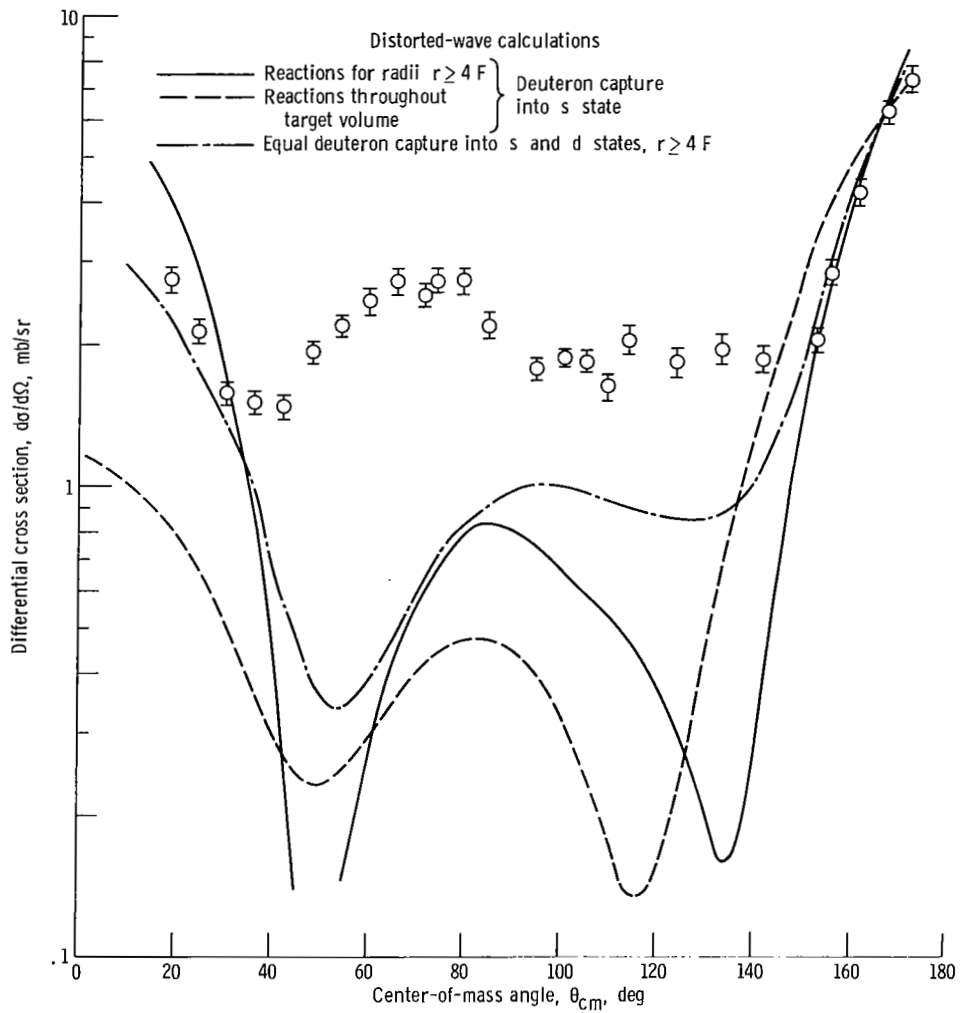Figure 7. – Differential cross section and polarization.

Figure 8. - Ground-state cross section for ^{3}He(α, p)^{6}Li. Isotopic spin, 0; $J^\pi = 1^+$; reaction Q-value, -4.02 MeV; incident energy, 42 MeV.

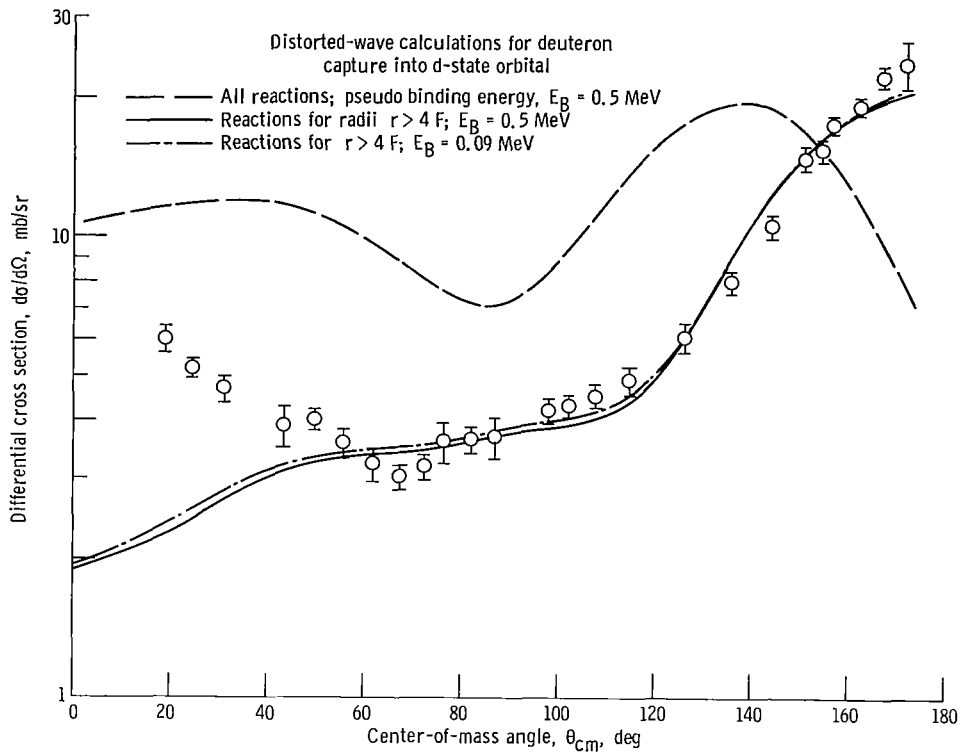Figure 9. – First-excited-state cross section for ^{3}He(α, p)^{6}Li. Isotopic spin, 0; $J^\pi = 3^+$; reaction Q-value, -6.20 MeV; incident energy, 42 MeV.
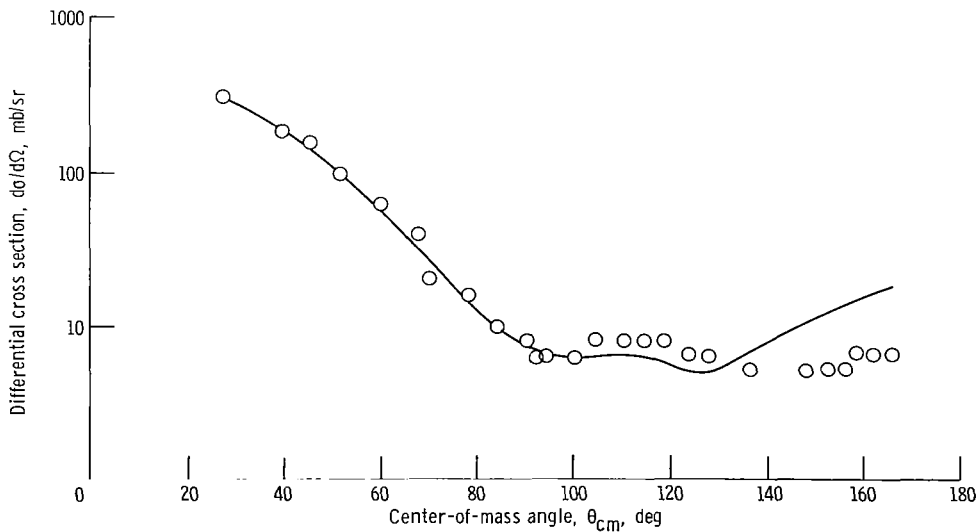

Figure 10. – Differential cross section for ^{6}Li(p, p)^{6}Li. Incident proton energy, 19.6 MeV. Real part of optical potential, 49.6 MeV; radius of real form factor, 1.25; diffuseness, 0.53 fermi. Absorptive part of optical potential, 6.8 MeV; radius of absorptive form factor, 1.25; diffuseness, 0.45 fermi. (Data from ref. 24.)

FIRST CLASS MAIL

"The aeronautical and space activities of the United States shall be conducted so as to contribute . . . to the expansion of human knowledge of phenomena in the atmosphere and space. The Administration shall provide for the widest practicable and appropriate dissemination of information concerning its activities and the results thereof."

— NATIONAL AERONAUTICS AND SPACE ACT OF 1958

NASA SCIENTIFIC AND TECHNICAL PUBLICATIONS

TECHNICAL REPORTS: Scientific and technical information considered important, complete, and a lasting contribution to existing knowledge.

TECHNICAL NOTES: Information less broad in scope but nevertheless of importance as a contribution to existing knowledge.

TECHNICAL MEMORANDUMS: Information receiving limited distribution because of preliminary data, security classification, or other reasons.

CONTRACTOR REPORTS: Scientific and technical information generated under a NASA contract or grant and considered an important contribution to existing knowledge.

TECHNICAL TRANSLATIONS: Information published in a foreign language considered to merit NASA distribution in English.

SPECIAL PUBLICATIONS: Information derived from or of value to NASA activities. Publications include conference proceedings, monographs, data compilations, handbooks, sourcebooks, and special bibliographies.

TECHNOLOGY UTILIZATION PUBLICATIONS: Information on technology used by NASA that may be of particular interest in commercial and other non-aerospace applications. Publications include Tech Briefs, Technology Utilization Reports and Notes, and Technology Surveys.

Details on the availability of these publications may be obtained from:

SCIENTIFIC AND TECHNICAL INFORMATION DIVISION
NATIONAL AERONAUTICS AND SPACE ADMINISTRATION
Washington, D.C. 20546